Published in final edited form as:
Free Radic Biol Med. 2015 February ; 79: 56–68. doi:10.1016/j.freeradbiomed.2014.11.016.

Increased Mitochondrial Pro-oxidant Activity Mediates Up-regulation of Complex I S-glutathionylation via Protein Thiyl Radical in the Murine Heart of eNOS$^{-/-}$

Patrick T. Kang, **Chwen-Lih Chen**, and **Yeong-Renn Chen**
Department of Integrative Medical Sciences, College of Medicine, Northeast Ohio Medical University, Rootstown, OH 44272

Abstract

In response to oxidative stress, mitochondrial Complex I is reversibly S-glutathionylated. We hypothesized that protein S-glutathionylation (PrSSG) of Complex I is mediated by a kinetic mechanism involving reactive protein thiyl radical (PrS$^{\bullet}$) and GSH *in vivo*. Previous studies have shown that *in vitro* S-glutathionylation of isolated Complex I at the 51 kDa and 75 kDa subunits was detected under the conditions of $^{\bullet}O_2^-$ production, and mass spectrometry confirmed that formation of Complex I PrS$^{\bullet}$ mediates PrSSG. Exposure of myocytes to menadione resulted in enhanced Complex I PrSSG and PrS$^{\bullet}$ (Kang *et al Free Radical Biol. Med.* 2012; 52: 962–73). In this investigation, we tested our hypothesis in the murine heart of eNOS$^{-/-}$. The eNOS$^{-/-}$ mouse is known to be hypertensive and develops the pathological phenotype of progressive cardiac hypertrophy. The mitochondria isolated from the eNOS$^{-/-}$ myocardium exhibited a marked dysfunction with impaired state 3 respiration, a declining respiratory control index, and decreasing enzymatic activities of ETC components. Further biochemical analysis and EPR measurement indicated defective aconitase activity, a marked increase in $^{\bullet}O_2^-$ generation activity, and a more oxidized physiological setting. These results suggest increasing prooxidant activity and subsequent oxidative stress in the mitochondria of the eNOS$^{-/-}$ murine heart. When Complex I from the mitochondria of the eNOS$^{-/-}$ murine heart was analyzed by immuno-spin trapping and probed with anti-GSH antibody, both PrS$^{\bullet}$ and PrSSG of Complex I were significantly enhanced. Overexpression of SOD2 in the murine heart dramatically diminished the detected PrS$^{\bullet}$, supporting the conclusion that mediation of Complex I PrSSG by oxidative stress-induced PrS$^{\bullet}$ is a unique pathway for the redox regulation of mitochondrial function *in vivo*.

Keywords

Mitochondria; eNOS$^{-/-}$ murine heart; Complex I; S-glutathionylation; Protein thiyl radical; Oxidative stress

*To whom correspondence should be addressed: Yeong-Renn Chen, Department of Integrative Medical Sciences, College of Medicine, Northeast Ohio Medical University, 4209 State Route 44, Rootstown, OH 44272, USA, Tel.: (330) 325-6537; Fax: (330) 325-5912; ychen1@neomed.edu.

INTRODUCTION

Mitochondria are the major source of oxygen free radical production. In mitochondria, the generation of $^{\bullet}O_2^-$ and $^{\bullet}O_2^-$-derived oxidants can act as a redox signal in triggering cellular events such as apoptosis, proliferation, and senescence. The mitochondrial redox pool is enriched in GSH; overproduction of $^{\bullet}O_2^-$ and $^{\bullet}O_2^-$-derived oxidants decreases the ratio of GSH to GSSG [1]. Complex I is the major component of the ETC that hosts protein redox thiols. It has been documented that the 51 kDa and 75 kDa subunits from the hydrophilic domain of Complex I are involved in redox modification of S-glutathionylation *in vitro* and *in vivo* [2–7]. *In vitro* studies using isolated mitochondria indicate that increasing Complex I S-glutathionylation is favored under conditions of oxidative stress such as exposure to organic peroxide [2, 3], the thiol oxidant diamide [5], or overproduction of $^{\bullet}O_2^-$ [7]. *In vitro* studies also support the conclusion that the molecular mechanism of Complex I S-glutathionylation can be mediated by the thermodynamic mechanism controlled by GSSG [3, 4] or a kinetic mechanism controlled by protein thiyl radicals in the presence of GSH [7].

The mitochondria of the cardiovascular system are an important target for the NO generated by nitric oxide synthase (NOS). NO serves as a physiological regulator of mitochondrial respiration [8–11]. Under physiological conditions of low O_2 tension, NO competes with O_2 in reversibly binding to the heme a_3-Cu_B of cytochrome *c* oxidase (C*c*O or Complex IV), thus decreasing the rate of ADP-independent O_2 consumption and subsequently alleviating $^{\bullet}O_2^-$ production [12, 13].

The NO produced by eNOS functions as one of the paracrine factors for endothelial cell to cardiomyocyte communication [14], including a role in limiting cardiac hypertrophy. The $eNOS^{-/-}$ mouse develops the phenotypes of hypertension [15], increasing contractile response to β-agonists such as isoproterenol [15–18], and progressive cardiac hypertrophy [19]. In the angiotensin type II (AT_2) receptor deletion mouse, decreased eNOS expression has been linked to the hypertrophic effect in cardiac remodeling [20]. Numerous studies further indicate an anti-hypertrophic role for NO in cardiomyocytes [21] and in the whole heart [22, 23]. The eNOS-deficient mouse displayed exacerbated left ventricular hypertrophy and dysfunction after imposition of pressure overload [22, 23], while cardiomyocyte-specific overexpression of eNOS attenuated left ventricular hypertrophy after pressure overload [24]. In the mouse model of pressure overload-induced cardiac hypertrophy, increased $^{\bullet}O_2^-$ by eNOS uncoupling has been linked to promoting cardiac hypertrophy [25].

In the post-ischemic murine heart, eNOS knockout results in a decrease in the oxygen tension (pO_2) in the myocardium, increasing the oxygen consumption rate (OCR) by mitochondria and reducing the formation of peroxynitrite ($OONO^-$) [26, 27]. It is well known that NO traps $^{\bullet}O_2^-$ to form $OONO^-$ at a very fast rate ($k \sim 10^9$–10^{10} $M^{-1}s^{-1}$). Therefore, eNOS-derived NO modulates post-ischemic oxygen consumption *via* the formation of excess $OONO^-$, subsequently impairing mitochondrial function during reperfusion [26, 27].

We hypothesize that the absence of eNOS-derived NO will increase pro-oxidant activity and subsequent oxidative stress in the mitochondria of the myocardium, altering mitochondrial function and redox status, and enhancing protein S-glutathionylation of Complex I *via* the kinetic mechanism involving protein thiyl radical intermediates.

There is a lack of systematic investigation directed toward understanding how eNOS-derived NO mediates mitochondrial function and redox status in the myocardium under physiological conditions. Determination of the above mechanism is of importance because of the implications for its regulation in cardiovascular disease and the physiological setting of mitochondrial redox. Therefore, we have performed studies to characterize the mitochondrial function and its redox biochemistry from the $eNOS^{-/-}$ murine heart. We report that the absence of NO produced by eNOS increases oxidative stress in mitochondria of the myocardium and enhances protein thiyl radical-dependent S-glutathionylation of Complex I.

MATERIAL AND METHODS

Animals

The $eNOS^{-/-}$ (B6.129P2-*Nos3*$_{tm1Unc}$/J), SOD2-tg (FVB-Tg(Myh6-SOD2,Tyr)3Pne/J) and the corresponding wild type (WT) background mice (C57BL6/J and FVB/NJ) were purchased from the Jackson Lab. Male, age-matched mice (16 – 18 weeks old for $eNOS^{-/-}$/WTB6, 12 – 14 weeks old for SOD2-tg/WTNJ) were used in this study. All procedures were performed with the approval of the Institutional Animal Care and Use Committee at Northeast Ohio Medical University (Rootstown, OH) and conformed to the *Guide for the Care and Use of Laboratory Animals* as adopted and promulgated by NIH.

Reagents

Glutathione (GSH), diphenyleneiodonium (DPI), 5,5'-dithio bis-2-nitrobenzoic acid (DTNB, Ellman′s reagent), diethylenetriaminepentaacetic acid (DTPA), ubiquinone-1 (Q_1), sodium cholate, deoxycholic acid, rotenone, polyethylene glycol-linked superoxide dismutase (PEG-SOD), β-nicotinamide adenine dinucleotide (reduced form, NADH), β-nicotinamide adenine dinucleotide phosphate (reduced form, NADPH), L-NG-nitroarginine methyl ester (L-NAME), 1-Oxyl-2,2,6,6-tetramethyl-4-hydroxypiperidine (TEMPOL), glutathione reductase (GR), and other general chemicals were purchased from Sigma Chemical Company (St. Louis, MO) and used as received. The 5,5-dimethyl-1-pyrroline-*N*-oxide (DMPO) spin trap was purchased from Dojindo Molecular Technologies, Inc. (Rockville, MD), and stored under argon at −80 °C until needed. The anti-GSH monoclonal antibody was purchased from ViroGen (Watertown, MA). The spin probe 1-hydroxy-3-methoxycarbonyl-2,2,5,5-tetramethylpyrrolidine.HCl (CM-H) and the anti-DMPO polyclonal antibody were purchased from Enzo Life Sciences Inc. (Farmingdale, NY). The anti-eNOS, anti-GAPDH, antiaconitase, anti-Rieske iron-sulfur protein, anti-Cox I, and anti-SOD2 antibodies were purchased from Santa Cruz Biotechnology Inc. (Dallas, TX).

Preparation of mitochondria

Mitochondria were prepared from the murine myocardium by the differential centrifugation method according to our published protocol [28, 29]. Briefly, the mouse heart was homogenized in 1 mL of M-buffer (in mM, mannitol 230, sucrose 70, EDTA 1, EGTA 1, and Trizma 5, pH 7.4) containing 1 unit of nagarse (Sigma-Aldrich, St. Louise, MO) on ice. The cOmplete protease inhibitor cocktail (1 ×, Roche Life Science, Indianapolis, IN) and PMSF (phenylmethanesulfonylfluoride, 1 mM in DMSO) were added to the homogenate after a 5-min incubation. The resulting homogenate was subsequently centrifuged 500 × g for 5 min to remove debris, and a second centrifugation of supernatant at 20,000 × g for 10 min yielded mitochondria sediment. The mitochondrial pellet was re-suspended in M-buffer and the protein concentration was determined by the Lowry method using bovine serum albumin as a standard. The cytosolic contamination was evaluated by immunoblotting the mitochondrial preparations using a monoclonal antibody (1:500) against glyceraldehyde 3-phosphate dehydrogenase (GAPDH, a housekeeping cytosolic protein, Santa Cruz Biotechnology, Inc., Dallas, TX); blotting of cytosolic preparations served as a positive control.

Analytical methods

Optical spectra were measured on a Shimadzu 2600 UV/Vis recording spectrophotometer. The concentrations of Q_1 and Q_2 were determined by absorbance spectra from $NaBH_4$ reduction using a millimolar extinction coefficient $\varepsilon_{(275nm\text{-}290nm)} = 12.25\ mM^{-1}cm^{-1}$ [30]. The electron transfer activities of Complexes I-IV from the heart mitochondrial preparation were assayed by our published methods [31]. The enzymatic activity of aconitase in mitochondria was assayed by measuring the conversion of citrate to α-ketoglutarate in the presence of isocitrate dehydrogenase by the absorbance increase at 340 nm at 37 °C. An appropriate amount of mitochondrial preparation (permeabilized by alamethicin at a 40 μg mitochondrial protein: 1 μg alamethicin ratio) was added to the assay mixture (to a final volume of 1 mL, containing in mM: Tris-HCl 50, cysteine 1, sodium citrate 1, $MnCl_2$ 0.5, NADP 0.2, pH 7.4), and the reaction was initiated with isocitrate dehydrogenase (2 units/mL).

Measurement of the oxygen consumption rate (OCR) of Mitochondrial Preparations

Mitochondrial respiration was measured by the polarographic method using a Clark-type oxygen electrode (Oxytherm, Hansatech Instruments, Norfolk, England) at 30 °C and reported in nmol/min. The NADH-linked respiration buffer contained glutamate/malate (in mM, potassium glutamate 140, NaCl 10, $MgCl_2$ 1, EGTA 1, malate 5, Trizma 1, phosphate 2.5, and cytochrome *c* 0.01, adjusted to pH 7.4). Mitochondrial preparations were added to the respiration buffer to a final concentration of 0.6 mg/mL. OCR (NADH-linked) was measured as follows: state 2, OCR of mitochondrial preparations with glutamate/malate; state 3, OCR stimulated by ADP (200 μM); state 4, OCR after the addition of oligomycin (2 μg/mL) following ADP addition; uncoupled respiration, OCR after the addition of FCCP (2.5 μM) following oligomycin. The oxygen electrode was calibrated at 1 atm by assuming the concentration of O_2 in the respiration buffer at 30 °C to be 230 μM.

Measurement of the mitochondrial state 3 ATP generation rate

The mitochondrial ATP flux (accumulation of ATP within 1 min) was measured using an ATP Bioluminescent Assay Kit (Sigma-Aldrich, St. Louis, MO) following the manufacturer ′s protocol. The mitochondrial state 3 oxygen consumption rate was simultaneously measured on the Oxytherm under the conditions as previously described. Briefly, the mitochondrial preparation (to a final concentration of 0.6 mg/mL) was added to the NADH-linked respiration buffer, and ADP (to a final concentration of 1 mM) was subsequently added. Reaction mixture (5 μL) was withdrawn from the reaction chamber and immediately added to 495 μL of pre-heated ATP-assay buffer (70 °C, 10 min) as the initial ATP concentration. Another 5 μL of reaction mixture was sampled 60-sec after the initial sampling as the final ATP concentration. The linear oxygen consumption rate during the ATP sampling time span was ensured by the simultaneous oxygen polarography monitoring. The bioluminescent signal was recorded on the OrionL microplate luminometer (Titertek-Berthold Detection Systems GmbH, Pforzheim, Germany).

Measurement of mitochondrial $^{\bullet}O_2^-$ production by EPR spin trapping

EPR measurements of $^{\bullet}O_2^-$ generation by isolated mitochondria were carried out on a Bruker EMX Micro spectrometer operating at 9.43 GHz with 100 kHz modulation frequency at room temperature [7]. The reaction mixture containing the NADH-linked respiration buffer supplemented with DTPA (1 mM) /DMPO (100 mM) was mixed with the mitochondrial preparation (to a final 0.6 mg protein/mL) at 30 °C for 4 min. The reaction mixture was then transferred into a 50-μL capillary (Drummond Wiretrol, Broomall, PA), sealed, loaded into the EPR resonator (HS cavity, Bruker Instrument, Billerica, MA), equilibrated to 298 K, and tuned within 2 min. The scan of the EPR spectrum was started at exactly 6 min after the initial reaction. Parameters: center field 3360 G, sweep width 100 G, power 20 mW, receiver gain 1×10^5, modulation amplitude 1 G, conversion time 40.96 ms, time constant 163.84 ms, number of scans: 5. The spectral simulations were performed using the WinSim program developed at NIEHS by Duling [32].

Glutathione recycling method

The amount of reduced and oxidized glutathione (GSH and GSSG) in mitochondria was determined by the glutathione recycling method [33, 34]. In this method, the reaction rates of excess glutathione reductase (GR), NADPH, and DTNB were limited by the presence of GSH and GSSG. Isolated mitochondria, as well as a series of known concentrations of GSH and GSSG, were mixed with 5-sulfosalicylic acid (5-SSA, 5%) in the presence of Triton X-100 (0.3%). The protein mixture was subjected to precipitation by centrifugation (12,000 rpm × 2 min at 4 °C). The supernatant was divided into two portions: one portion (room temperature, RT) for additional GSH-quenching and another portion (sitting on ice) ready for total [GSH+GSSG] determination. For the GSH-quenching, an excess amount of 2-vinylpyridine (2-VP, to a final concentration of 2%) was added to the mixture after adjusting the pH to 6~7 with triethanolamine. The mixture was incubated at RT for 2 hr. The reduced GSH was thus blocked by 2-vinylpyridine and the remaining oxidized GSSG was ready for measurement. Standard concentrations of GSH and GSSG undergoing the same 5-SSA/2-VP treatment were used to create a linear regression standard curve. The above standards/

samples were added into glutathione reaction buffer (in mM, potassium phosphate 50, pH 7.5, EDTA 1, DTNB 0.6, NADPH 0.1, 30 °C), and the reaction was started by the addition of GR enzyme (2 units/mL for the detection of [GSH + GSSG], and 0.4 units/mL for the detection of [GSSG]). The assay was monitored by absorbance increase at 412 nm following the reduction of DTNB (ε_{412nm} = 13.6 mM^{-1} cm^{-1}). The concentrations of GSH + GSSG as well as GSSG were calculated by interpolation from the standard curves.

Immunoblotting analysis

The reaction mixture was mixed with Laemmli sample buffer at a ratio of 4:1 (v/v), incubated at 70 °C for 10 min, and then loaded onto a 4–12 % Bis-Tris polyacrylamide gradient gel. Samples were run at RT for 50 min at 190 V. Protein bands were electrophoretically transferred to a nitrocellulose membrane in 25 mM Bis-Tris, 25 mM Bicine, 0.029% (w/v) EDTA, and 10% methanol. Membranes were blocked for 1 hr at RT in Tris-buffered saline (TBS) containing 0.1% Tween-20 (TTBS) and 5% dry milk (BioRad, Hercules, CA). The blots were then incubated overnight with primary antibody at 4 °C. Blots were then washed 3 times in TTBS, and incubated for 1 hr with horseradish peroxidase-conjugated secondary antibody in TTBS at RT. The blots were again washed twice in TTBS and twice in TBS, and then visualized using ECL Western Blotting Detection Reagents (GE Healthcare Life Sciences, Fairfield, CT).

Data analysis

All data were reported as group averages. Statistical analysis was performed using Origin 9.1 data analysis software. Results were presented as mean ± SEM, followed by group number (*n*), and p value. Comparisons between two groups (the data sets of Figs. 1, 2, 4, 5, and 6) were assessed by student's t-test to analyze the significance of differences. Comparisons among multiple groups (the data set of three groups in Fig. 1B and the data set of four groups in Fig. 2B) were assessed by one-way ANOVA followed by Tukey's post hoc tests. A probability value of $p < 0.05$ was used to establish statistical significance.

RESULTS

Impairment of mitochondrial function in the myocardium of $eNOS^{-/-}$ mice

Tissue homogenates of the aorta from $eNOS^{-/-}$ mice were immunoblotted with anti-eNOS antibody to confirm eNOS deletion *in vivo* (supplementary Fig. 1a). To test the oxidative stress hypothesis, studies were performed in the $eNOS^{-/-}$ mouse (males, 16 – 18 weeks old). Age- and gender-matched wild-type mice (C57Bl/6 background) were used as controls. Mitochondria were prepared from the murine myocardium by differential centrifugation, and then subjected to oxygen consumption measurements. Isolated mitochondrial preparations and cytosol fractions were immunoblotted with anti-GAPDH antibody, and the absence of the GAPDH signal in the mitochondrial preparations ensured that isolated mitochondria were free of cytosolic contamination (supplementary Fig. 1b). Fig. 1A shows a typical profile of oxygen consumption in mitochondria from the myocardia of wild type and $eNOS^{-/-}$ mice. State 3 (ADP-dependent) and state 4 (ADP-independent) respiration of mitochondrial preparations was measured by oxygraph. The NADH-linked and ADP-stimulated O_2 consumption rate (state 3) declined from 123.4 ± 3.9 to 90.2 ± 3.2 (in nmol

O_2/min/mg protein, WT (B6) *vs* eNOS$^{-/-}$ mouse, $n = 7$, $p < 0.001$, in Fig. 1B). The ADP-independent O_2 consumption rate (state 4) increased from 15.5 ± 0.7 to 24.4 ± 1.3 ($n = 7$, $p < 0.001$, Fig. 1B). Mediation of ATP production by the mitochondria from eNOS$^{-/-}$ myocardia decreased from 292.2 ± 24.2 to 223.0 ± 23.4 (in nmol ATP production/min/mg protein, $n = 5$, $p < 0.05$, in Fig. 1D) as analyzed by ATP-luciferase chemiluminescence assay. The respiratory control index (RCI, defined as the ratio of state 3 to state 4) decreased from 8.1 ± 0.6 to 3.8 ± 0.3 ($n = 7$, $p < 0.001$) as indicated in Fig. 1C. These data confirm that the mitochondrial integrity in the myocardium was impaired in the absence of eNOS, supporting the regulatory role of NO generated by eNOS in mitochondrial respiration in the myocardium.

To assess the maximal electron transfer activity of isolated mitochondria, FCCP (2.5 μM) was added to uncouple the mitochondria and maximize the respiratory capacity. We observed that the NADH driven FCCP-uncoupled O_2 consumption rate was significantly decreased from 150.3 ± 4.3 to 113.2 ± 5.2 ($n = 7$, $p < 0.001$, Fig. 1B), suggesting that ETC activity mediating the OCR was impaired by eNOS deletion.

Enhancement of mitochondria-mediated $^{\bullet}O_2^-$ generation in the myocardium of eNOS$^{-/-}$ mice

The production of $^{\bullet}O_2^-$ mediated by isolated mitochondria in different respiratory states was induced by glutamate/malate (NADH-linked), and measured by EPR spin-trapping with DMPO. A SOD-dependent four-line spectrum of DMPO/$^{\bullet}$OH was detected, indicating that $^{\bullet}O_2^-$ generation was mediated by the mitochondria of the mouse heart under conditions of state 2 respiration (Fig. 2A, *b*). Addition of ADP (state 3 respiration) diminished mitochondria-mediated $^{\bullet}O_2^-$ generation by ~65%, a significant decrease indicating that coupling of enhanced O_2 consumption with oxidative phosphorylation for ATP synthesis decreased the e^- leakage to molecular oxygen (Fig. 2A, *c*). In the presence of oligomycin A (state 4 respiration), mitochondria-mediated $^{\bullet}O_2^-$ generation induced by glutamate/malate was not decreased by the addition of ADP (Fig. 2B, *state 2 versus state 4*), presumably due to decreased OCR and restoring the electrochemical gradient (Δp).

We next assayed the $^{\bullet}O_2^-$ generation activity mediated by mitochondria isolated from the hearts of eNOS$^{-/-}$ mice. We observed that NADH-linked $^{\bullet}O_2^-$ production by mitochondria was consistently increased under the conditions of states 2–4. In the presence of ADP (state 3), NADH-linked $^{\bullet}O_2^-$ production was enhanced to 148.8 ± 8.3% ($n = 6$, $p < 0.01$) (Fig. 2B, *gray bar*), supporting the hypothesis that mitochondrial dysfunction occurring in the eNOS$^{-/-}$ mouse heart is caused by impaired state 3 OCR and overproduction of oxygen free radicals.

Aconitase activity in mitochondria was reported to be a redox sensor of reactive oxygen species [35–37]. The reaction of aconitase with $^{\bullet}O_2^-$ ($k \sim 10^7\ M^{-1}s^{-1}$) rapidly inactivates its enzymatic activity by producing an inactive [3Fe-4S] cluster (g=2.018), free iron (II), and H_2O_2. Consequently, inactivation of mitochondrial aconitase by $^{\bullet}O_2^-$ facilitates the formation of hydroxyl radicals via a Fenton-type mechanism [38]. Accordingly, we have further detected a marginal decline in the enzymatic activity of aconitase to 67.9 ± 3.2% (*vs* mitochondrial aconitase of wild type mice, $n = 6$, $p < 0.001$) in the mitochondria of the

eNOS$^{-/-}$ mouse heart (Fig. 2C), corroborating increased mitochondrial $^{\bullet}O_2^-$ production in the eNOS$^{-/-}$ mouse myocardium. There was no significant difference in protein expression levels of aconitase in the mitochondria between wild type and eNOS$^{-/-}$ as measured by immunoblotting (Fig. 2D), indicating oxidative impairment of aconitase in the eNOS$^{-/-}$ mouse heart.

Redox status in the myocardium of eNOS$^{-/-}$ mice

We used X-band EPR to analyze the redox status of the myocardium during the oxidation of CM-H (a spin probe of cyclic hydroxylamine) to a stable nitroxide in myocardium tissue homogenate. Under non-energized conditions (without external NADH or succinate stimulation), the redox activity of wild type myocardium was 2.66 ± 0.12 nmol nitroxide produced/min/mg protein of tissue homogenate (based on spin quantitation, $n = 3$). In eNOS$^{-/-}$ mice, the physiological redox setting of the myocardium was more oxidized and less reduced, based on a higher activity of conversion of CM-H to stable nitroxide (increased by 41%, Fig. 3A) and lower TEMPOL reduction (decreased by 26%, Fig. 3B). This result corroborates the data from EPR spin trapping with DMPO shown in Fig. 2B.

Oxidative impairment of the mitochondrial ETC in the eNOS$^{-/-}$ myocardium

Mitochondria isolated from mouse hearts were subjected to an assay of enzymatic activities of the respiratory complexes. In the myocardium of eNOS$^{-/-}$ mice, the enzymatic activities of the electron transport complexes (complexes I-IV) declined ($n = 7$, $p < 0.001$, Fig. 4A), consistent with the detection of an impaired FCCP-mediated uncoupling of the O_2 consumption rate (Fig. 1B). There were no significant alterations in protein expression of the mitochondrial ETC (Fig. 4B). Immunoblotting analysis also indicated a slight reduction in the protein expression of SOD2 (by ~15%, $n = 4$) from the mitochondria of eNOS$^{-/-}$ mice, supporting increased $^{\bullet}O_2^-$ production and oxidative impairment of the ETC in the mitochondria of the eNOS$^{-/-}$ murine heart.

Effect of L-NAME treatment on the mitochondrial function of the murine heart

The above results were evaluated with pharmacological inhibition of NO synthase *in vivo* using L-NAME. In wild type mice, oral administration of the NOS inhibitor, (L-NAME, 1 mM in drinking water), induced arterial hypertension and microvascular lesions linked to up-regulation of oxidative stress [39, 40]. Here, mitochondria isolated from the myocardium of L-NAME-treated mice exhibited a modest decrease in state 3 respiration (by 12.6%), but showed a substantial enhancement of state 4 respiration (by 82%, $n = 9$, $p < 0.001$) and thus a significant reduction of the respiratory control index (from 8.3 ± 0.6 to 4.7 ± 0.4, $n = 9$, $p < 0.001$) indicated in the supplementary Fig. 2 (A–C). In addition, impaired enzymatic activities of Complexes I, II, and IV and aconitase (by 20–35%) were detected in the mitochondria of mice after LNAME treatment (supplementary Fig. 2D), indicating increased oxidative impairment in the mitochondria due to inhibition of NO generation *in vivo*. The redox status of the myocardium from L-NAME-treated mice showed a 21.8% elevation in the redox activity of converting CM-H to a stable nitroxide (supplementary Fig. 2E). NADH-linked $^{\bullet}O_2^-$ production by the mitochondria isolated from L-NAME-treated mice was enhanced under the condition of state 3 respiration (by 28.8 ± 3.8%, $n = 9$, $p < 0.01$ in

the supplementary Fig. 2F), supporting the conclusion that L-NAME mediated mitochondrial dysfunction in the myocardium was caused by increased $^{\bullet}O_2^-$ and impaired mitochondrial integrity.

Redox alterations in the GSH pool and S-glutathionylation of Complex I

The genetic deletion of eNOS resulted in significantly enhanced pro-oxidant activity in the mitochondrial fraction of the myocardium. We determined GSH and GSSG levels quantitatively by the enzymatic recycling method, observing (i) a significant elevation of GSSG levels in the mitochondrial preparation (from 0.104 ± 0.006 to 0.138 ± 0.010 nmol/mg protein, $n = 8$, $p < 0.01$), and (ii) a marginal down-regulation in the GSH/GSSG ratio of the mitochondria (from 31.8 to 26.2) as shown in Table I. These results were basically consistent with a modest increase in the oxidative stress in the mitochondria of the $eNOS^{-/-}$ murine heart. However, the GSH pool in the cytosolic fraction of $eNOS^{-/-}$ myocardium was not changed significantly.

We would expect a depression in the GSH/GSSG ratio from $eNOS^{-/-}$ myocardial mitochondria to increase the status of S-glutathionylation of the mitochondrial Complex I. To test this hypothesis, we used polyclonal antibodies against Complex I, Ab51 and Ab75 [6, 41], to immunoprecipitate the 51 kDa- and 75 kDa-subunits of Complex I from mitochondrial preparations, followed by immunoblotting with an anti-GSH monoclonal antibody. As indicated in Fig. 5, in the $eNOS^{-/-}$ myocardium, the detected Complex I-derived S-glutathionylation on the 51 kDa and 75 kDa subunits of Complex I was enhanced to 199.3 ± 21.6% and 137.5 ± 12.7% respectively. Although complex I glutathionylation within the mitochondria of $eNOS^{-/-}$ myocardium correlated with partial loss of activity (Fig. 4A), deglutathionylation of complex I with dithiothreitol (DTT) or β-mercaptoethanol did not restore complex I activity (data not shown).

Enhancement of Complex I-derived protein thiyl radicals in the mitochondria of the $eNOS^{-/-}$ murine heart

The redox signal regulating Complex I-derived S-glutathionylation has been hypothesized to involve reactive oxygen species and homeostasis of the GSH pool in mitochondria [7]. A kinetic mechanism, a reaction of protein reactive thiyl radical intermediates with GSH, is more likely to mediate enhanced S-glutathionylation of Complex I in the mitochondria of $eNOS^{-/-}$ mice. To test the hypothesis of a protein thiyl radical intermediate, immuno-spin trapping with an anti-DMPO polyclonal antibody was used to define Complex I-derived protein radical formation in mitochondria. Mitochondrial preparations were incubated with DMPO (200 mM), and the aliquots were subjected to SDS-PAGE and Western blotting using an anti-DMPO antibody. The immobilized nitrone adduct of Complex I was detected in the 51 kDa and 75 kDa subunits by immunoblotting (Fig. 6). In the mitochondria isolated from the $eNOS^{-/-}$ murine heart, the detected DMPO adduct of Complex I-derived protein radicals increased to 178.9 ± 34.7 and 253.0 ± 45.5% on the 51 kDa and 75 kDa subunits respectively (Fig. 6, bar graph insert).

To determine whether the cysteinyl residues were involved in the detected Complex I-derived protein radical adducts of DMPO in mitochondria, we tested the effects of DTNB

and GSH on the formation of DMPO protein radical adducts. Addition of DTNB to the reaction mixture containing mitochondria and DMPO diminished the signal intensity of DMPO adducts by 70.7 ± 12.6% (at the 51 kDa subunit) and 65.3 ± 3.8% (at the 75 kDa subunit), suggesting the cysteine thiols as the binding sites of DMPO (Fig. 7A–7B). When GSH (2 mM) was included in the reaction mixture to compete with DMPO in binding to the Complex I protein thiyl radicals, the signal intensity of DMPO adducts was decreased by 66.7 ± 5.9% (51 kDa subunit) and 49.3 ± 3.9% (75 kDa subunit); further confirming the involvement of cysteinyl residues in the protein radical formation of Complex I.

As indicated in Fig. 7C, pre-treatment of mitochondria (energized by glutamate plus malate) with DPI (diphenyleneiodonium, 1 mM) significantly enhanced the signal intensity of DMPO adducts up to 9.2-fold (51 kDa) and 1.7-fold (75 kDa). Presumably, DPI inhibition greatly increases electron leakage from the FMN cofactor and FMN-binding domain of the 51 kDa polypeptide, thus dramatically enhancing the Complex I protein radicals induced by $^{\bullet}O_2^-$ attack. The addition of GSH greatly diminished DPI-enhanced Complex I thiyl radicals (Upper panel in Fig. 7C), and subsequently increased the S-glutathionylation of Complex I (middle and lower panel in Fig. 7C), reinforcing the mechanism of protein thiyl radicals mediating S-glutathionylation of Complex I.

Overexpression of SOD2 in the myocardium suppresses the formation of Complex I-derived protein thiyl radicals

The proposed mechanism was further tested in a model of cardiac-specific SOD2 transgenic mice. The SOD2-tg mouse hemizygotes are viable, fertile, and normal in size. Transgenic expression of SOD2 is specific to the myocardium and localized to the mitochondria. Western analysis indicated enhanced SOD2 expression in the mitochondria of the murine heart up to 7-fold (Fig. 8A, upper panel, with subunit I of complex IV (COX I) as the loading control, $n = 6$). EPR spin trapping analysis further showed no detectable $^{\bullet}O_2^-$ generation by the mitochondria isolated from SOD2-tg myocardia (Fig. 8A, lower panel, *b* vs *e*) and significantly lower sensitivity to antimycin A treatment (Fig. 8A, lower panel, *c* vs *f*). The protein thiyl radicals of Complex I at the 51 kDa and 75 kDa subunits in the isolated mitochondria were further analyzed by the technique of immuno-spin trapping with anti-DMPO antibody. As indicated in Fig. 8B, Complex I-derived protein thiyl radicals were nearly eliminated in the mitochondria of the SOD2-tg murine heart. Presumably, overexpression of SOD2 in the myocardium eliminates $^{\bullet}O_2^-$-mediated oxidative stress in the mitochondria and subsequently decreases Complex I-derived protein thiyl radical formation.

DISCUSSION

Mitochondrial dysfunction in the myocardium of eNOS$^{-/-}$

The current study has demonstrated that eNOS deletion impacts heart function via mitochondrial dysfunction caused by impairing mitochondrial integrity, as indicated by a decline in the respiratory control index (Fig. 1C), and by decreasing the enzymatic activities of the electron transport chain (Fig. 4A). This result is further supported by the experiment using the mouse model of pharmacological inhibition of eNOS with L-NAME, showing

impaired mitochondrial integrity as indicated by a decreased respiratory control index (supplemental Fig. 2A–C).

It has been proposed that NO generated from endothelial cells has the capacity to modulate mitochondrial functions related to respiration and metabolism, and that mitochondria are an important target of endothelium-derived relaxant factor (EDRF) [8, 9, 42]. It is thus expected that eNOS deletion will impair EDRF-mediated respiratory regulation, leading to mitochondrial dysfunction. In the $eNOS^{-/-}$ mouse model, the above rationale has now been verified in the cardiovascular system. It is likely that direct crosstalk between endothelium and myocytes was mediated by diffusible NO [14], which subsequently regulated mitochondrial respiration via reversibly binding to Complex IV or regulated the Q-cycle mediated by Complex III [43]. A higher partitioning of NO into the mitochondrial membrane in the myocytes can greatly facilitate this physiological process [44], thus augmenting the ability of NO to control mitochondrial respiration in the murine heart. The process also can be facilitated by the high capillary density (3000–4000/mm^2) in the adult mammalian myocardium [45].

Another major factor leading to mitochondrial dysfunction in the $eNOS^{-/-}$ murine heart was likely hypertension-induced progressive hypertrophy secondary to NO modulation. As reported by Barouch *et al.*, mice with non-conditional eNOS deletion have developed hypertrophy by the age of 5 months [46].

Pro-oxidant activity of mitochondria and oxidative stress in the myocardium of $eNOS^{-/-}$ mice

Mitochondria are the major source of oxygen free radical generation in the cardiovascular system [47]. The major endogenous source of $^{\bullet}O_2^-$ and $^{\bullet}O_2^-$-derived oxidants, which are toxic products of respiration, is oxidative phosphorylation (OXPHOS). Mitochondrial dysfunction resulting from eNOS knockout has revealed impaired OXPHOS and impaired enzymatic activities of the ETC with a minor downregulation of SOD2 (Fig. 4), leading to augmented ETC-mediated $^{\bullet}O_2^-$ generation as evidenced by the EPR spin trapping assay (Fig. 2). To assess damage, we focused on aconitase, an iron-sulfur protein containing a 4Fe-4S cluster and involved in the TCA cycle for controlling the ratio $NADH/NAD^+$ and regulation of OXPHOS, since exposure of aconitase to oxidants renders the enzyme inactive. Loss of aconitase activity in biological samples treated with pro-oxidants has been interpreted as a measure of oxidative damage. Significant impairment of aconitase activity was detected in the mitochondria from the $eNOS^{-/-}$ murine heart (Fig. 2C). A noteworthy loss of Complex II activity resulted from eNOS deficiency (Fig. 4A). Complex II is the only mitochondrial enzyme involved in both the TCA cycle and the electron transport chain, so loss of its activity leads to increased mitochondrial oxidative stress and impaired function of the TCA cycle. It appears that loss of eNOS itself leads to increased pro-oxidant activity of mitochondria, augmenting $^{\bullet}O_2^-$ generation activity mediated by mitochondria, and exacerbating the progress of hypertrophy. These data can also partially explain why $eNOS^{-/-}$ mice display the pre-diabetic phenotype with defective mitochondrial β-oxidation, decreased energy expenditure, and development of insulin resistance [48].

Topology of enhanced $^{\bullet}O_2^-$ generation by the mitochondria of eNOS$^{-/-}$ murine heart

Since the anionic form of $^{\bullet}O_2^-$ is too strongly negatively charged to readily pass the inner membrane, enhanced $^{\bullet}O_2^-$ production mediated by the mitochondria of the eNOS$^{-/-}$ murine heart exhibited a distinct membrane sidedness or "topology." Current experimental evidence suggested that extra-mitochondrial $^{\bullet}O_2^-$ release (induced by glutamate/malate, and trapped by DMPO) detected by EPR (Fig. 2B) was likely mediated by the Q_o site located near the inter-membrane space [49]. The close proximity of the Q_o site of Complex III to the inter-membrane space would result in the inevitable release of a fraction of any Complex III-derived $^{\bullet}O_2^-$ to the cytoplasmic site, ready for DMPO trapping (Fig. 9). Additional evidence has indicated that PEG-SOD inhibited $^{\bullet}O_2^-$–dependent DMPO/•OH formation as mediated by NADH-energized mitochondria (Fig. 2A, *d*). Since PEG-SOD cannot penetrate the outer membrane of the mitochondria, this result further supported that $^{\bullet}O_2^-$ was trapped outside the mitochondria by DMPO. In any case, DMPO reacts with $^{\bullet}O_2^-$ with a low rate constant (30–70 $M^{-1}s^{-1}$ [50]); therefore DMPO cannot possibly compete with the SOD2 of the intra-membrane space. Experimental evidence has also supported the conclusion that the remaining increased electron leakage contributes to increased $^{\bullet}O_2^-$ released to the matrix side and consequent aconitase inhibition (Fig. 2C). Excess hydrogen peroxide derived from SOD2-mediated dismutation of $^{\bullet}O_2^-$ in the mitochondrial matrix also induces aconitase inhibition [49].

Redox status in the myocardium of eNOS$^{-/-}$ mice

The above results were further supported by the EPR assay using the spin probes cyclic hydroxylamine (CM-H) and organic nitroxide (TEMPOL), indicating an overall more oxidized physiological setting detected in the eNOS$^{-/-}$ murine heart versus its wild type (Fig. 3). It is conceivable that the redox alteration in the myocardium is the consequence of increased mitochondria-derived $^{\bullet}O_2^-$ generation activity resulting from eNOS deletion. The results corroborate the redox status of mitochondrial thiols in the eNOS$^{-/-}$ murine heart, showing a decreased mitochondrial GSH/GSSG ratio and elevated protein S-glutathionylation of Complex I (Table I and Fig. 5). No significant difference in the redox status was detected in the cytosolic GSH pool of eNOS$^{-/-}$ versus wild type mice (Table I). However, notably enhanced oxidation of GSH to GSSG was detected in both cytosolic and mitochondrial fractions of the myocardium from L-NAME-treated mice (Table I), reinforcing the specific role of eNOS in regulating the mitochondrial redox status of the mouse heart.

It has been documented that the oxidation of cyclic hydroxylamine is often dependent on $^{\bullet}O_2^-$ [50]. The presence of PEG-SOD significantly diminished the redox activities of wild type and eNOS$^{-/-}$ myocardia by 45.7 % and 40.9 %, respectively under non-energized and basal conditions, indicating $^{\bullet}O_2^-$–dependent redox activity for CM-H oxidation (in nmol nitroxide produced/min/mg protein) as 1.17 for WT and 1.53 for eNOS$^{-/-}$ myocardia. This result was basically corroborated with that of EPR spin-trapping with DMPO.

Mechanism of Complex I S-glutathionylation in the eNOS$^{-/-}$ murine heart

Reversible S-glutathionylation of Complex I may proceed spontaneously by a thermodynamic mechanism of protein thiol-GSSG disulfide exchange *in vitro* [3, 4].

However, achieving this thermodynamic equilibrium would require a marked decline in the intracellular GSH/GSSG ratio (*i.e.*, to a 1/1 ratio to drive 50% conversion of protein to glutathionylated form) [51, 52], which can occur only under extreme conditions. Pharmacologic inhibition of glutathione reductase 2 intensively increases mitochondrial GSSG/GSH ratio, enhancing S-glutathionylation of Complex I *in vivo* via thermodynamic mechanism [53]. In the myocardium of eNOS$^{-/-}$ mice, enhanced Complex I S-glutathionylation occurs at a relative high GSH/GSSG ratio (Table I); therefore, the mechanism of thiol-disulfide exchange is not likely. A kinetic mechanism, a reactive protein sulfhydryl intermediate with GSH, is more likely to mediate increased protein S-glutathionylation of Complex I caused by eNOS deletion.

The protein thiyl radical is one of the most relevant reactive sulfhydryl intermediates to facilitate *in vivo* S-glutathionylation of Complex I, as seen in the myocardium of eNOS$^{-/-}$ mice. With immunospin trapping with anti-DMPO antibody, protein thiyl radical adducts of Complex I at the 51 kDa and 75 kDa subunits can be detected in isolated mitochondria from the wild-type murine heart (Fig. 6). The result strongly supports the above hypothesis that protein thiyl radical mediates S-glutathionylation of Complex I *in vivo*. This hypothesis has also gained strong support from *in vitro* S-glutathionylation using isolated Complex I and the model of HL-1 myocytes in a previous publication [7], unequivocally demonstrating that the protein thiyl radicals are the key reactive intermediates for *in vivo* site-specific S-glutathionylation of Complex I [7]. In the eNOS$^{-/-}$ murine myocardium, increased Complex I-derived thiyl radical formation is expected to further mediate enhanced protein S-glutathionylation of Complex I *in vivo* (Figs 5–6). Experimental evidence from the mouse model of SOD2-tg clearly revealed a faded Complex I-derived thiyl radical formation *in vivo* resulting from SOD2 overexpression (Fig. 8B), further reinforcing the role of $^{\bullet}O_2^-$-induced protein thiyl radicals in mediating protein S-glutathionylation of Complex I from the eNOS$^{-/-}$ murine heart. Note that overexpressiong SOD2 did not significantly alter the level S-glutathionylation of Complex I in the mitochondria of SOD2-tg, implicating a basal level of Complex I S-glutathionylation is essential for maintaining the basal level of physiological redox setting. Moreover, L-NAME treatment did not enhance the level of *in vivo* S-glutathionylation of Complex I, underlining the unique role of eNOS.

The loss of Complex I activity from eNOS$^{-/-}$ mitochondria was not ameliorated by treatment with thiol reductant even if Complex I S-glutathionylation was reversed; that is, deglutathionylation did not lead to restoration of Complex I activity in the mitochondria of eNOS$^{-/-}$ myocardium. Similar results have been observed when Complex I S-glutathinylation was enhanced by treatment of mitochondria by diamide [5]. As reported in the previous study [7], the cys_{226} residue as a ligand involved in the [4Fe-4S] binding of the N4 center has been identified as the site of protein thiyl radical formation and subsequent Complex I S-glutathionylation *in vitro*. Therefore, the kinetic mechanism mediated by Complex I thiyl radical may lead to irreversible damage of its electron transport activity due to disruption of the iron-sulfur cluster [7].

CONCLUSION

The present studies provide insights regarding the mechanism of Complex I S-glutathionylation *in vivo* resulting from genetic deletion of eNOS. The underlying mechanism has been characterized by impaired mitochondrial membrane integrity, increased pro-oxidant activity of the mitochondria in myocytes, enhanced Complex I-derived thiyl radical formation, and associated S-glutathionylation of Complex I, as illustrated in Fig. 9. Genetic deletion of eNOS abolished NO bioavailability and decreased blood flow in the vasculature, which would decrease O_2 and respiratory substrate supply, and persistently induce hypertension. Persistent hypertension potentially increases oxidative stress in the mitochondria of the myocardium, and elevation of oxidative stress would impair mitochondrial integrity and decrease ATP synthesis, conditions that would favor the progress of cardiac hypertrophy. The enhanced Complex I-derived thiyl radicals and S-glutathionylation in the myocardium of $eNOS^{-/-}$ likely represent pathological markers caused by redox post-translational modification. The mechanism addressed here provides a useful concept for understanding the kinetic mechanism of protein S-glutathionylation *in vivo*. Recognition of this mechanism is valuable in understanding the fundamental basis for the way in which EDRF produced by eNOS regulates redox signaling in mitochondria.

Supplementary Material

Refer to Web version on PubMed Central for supplementary material.

ACKNOWLEDGMENT

This work was supported by National Institutes of Health Grant HL83237 (Y-RC).

Abbreviations

NOS	nitric oxide synthase
eNOS	endothelial NOS or NOS3
EDRF	endothelium-derived relaxant factor
SOD2	manganese-containing superoxide dismutase
NQR	NADH ubiquinone reductase, or mitochondrial Complex I
$^{\bullet}O_2^-$	superoxide anion radical
$OONO^-$	peroxynitrite
$PrS^{\bullet}$	protein thiyl radical
PrSSG	Protein S-glutathionylation
ETC	electron transport chain
OCR	oxygen consumption rate
RCI	respiratory control index
Q_1	ubiquinone-1

DMPO	5,5-dimethyl-1-pyrroline-*N*-oxide
FMN	flavin mononucleotide
FCCP	carbonyl cyanide-4-(trifluoromethoxy)phenylhydrazone
DTNB	5,5-dithiobis-2-nitrobenzoic acid
GSH	glutathione
DPI	Diphenyleneiodonium
L-NAME	L-nitro-arginine methyl ester
Ab	antibody
SDS-PAGE	SDS polyacrylamide gel electrophoresis
EPR	electron paramagnetic resonance
PBS	phosphate buffered saline

REFERENCES

1. Costa NJ, Dahm CC, Hurrell F, Taylor ER, Murphy MP. Interactions of mitochondrial thiols with nitric oxide. Antioxid Redox Signal. 2003; 5:291–305. [PubMed: 12880484]
2. Taylor ER, Hurrell F, Shannon RJ, Lin TK, Hirst J, Murphy MP. Reversible glutathionylation of complex I increases mitochondrial superoxide formation. J Biol Chem. 2003; 278:19603–19610. [PubMed: 12649289]
3. Beer SM, Taylor ER, Brown SE, Dahm CC, Costa NJ, Runswick MJ, et al. Glutaredoxin 2 catalyzes the reversible oxidation and glutathionylation of mitochondrial membrane thiol proteins: implications for mitochondrial redox regulation and antioxidant DEFENSE. J Biol Chem. 2004; 279:47939–47951. [PubMed: 15347644]
4. Chen CL, Zhang L, Yeh A, Chen CA, Green-Church KB, Zweier JL, et al. Site-specific S-glutathiolation of mitochondrial NADH ubiquinone reductase. Biochemistry. 2007; 46:5754–5765. [PubMed: 17444656]
5. Hurd TR, Requejo R, Filipovska A, Brown S, Prime TA, Robinson AJ, et al. Complex I within oxidatively stressed bovine heart mitochondria is glutathionylated on Cys-531 and Cys-704 of the 75- kDa subunit: potential role of CYS residues in decreasing oxidative damage. J Biol Chem. 2008; 283:24801–24815. [PubMed: 18611857]
6. Chen J, Chen C, Rawale S, Chen C, Zweier J, Kaumaya P, et al. Peptide-based antibodies against glutathione-binding domains suppress superoxide production mediated by mitochondrial complex I. J Biol Chem. 2010; 285:3168–3180. [PubMed: 19940158]
7. Kang P, Zhang L, Chen C, Chen J, Green K, Chen Y. Protein thiyl radical mediates S-glutathionylation of complex I. Free Radical in Biology and Medicine. 2012; 53:962–973.
8. Moncada S, Erusalimsky JD. Does nitric oxide modulate mitochondrial energy generation and apoptosis? Nat Rev Mol Cell Biol. 2002; 3:214–220. [PubMed: 11994742]
9. Ramachandran A, Levonen AL, Brookes PS, Ceaser E, Shiva S, Barone MC, et al. Mitochondria, nitric oxide, and cardiovascular dysfunction. Free radical biology & medicine. 2002; 33:1465–1474. [PubMed: 12446203]
10. Erusalimsky JD, Moncada S. Nitric oxide and mitochondrial signaling: from physiology to pathophysiology. Arterioscler Thromb Vasc Biol. 2007; 27:2524–2531. [PubMed: 17885213]
11. Brown GC, Borutaite V. Nitric oxide and mitochondrial respiration in the heart. Cardiovasc Res. 2007; 75:283–290. [PubMed: 17466959]
12. Lamas S, Perez-Sala D, Moncada S. Nitric oxide: from discovery to the clinic. Trends in Pharmacological Sciences. 1998; 19:436–438. [PubMed: 9850605]

13. Brown GC. Nitric oxide and mitochondrial respiration. Biochimica et biophysica acta. 1999; 1411:351–369. [PubMed: 10320668]
14. Zhang M, Shah AM. ROS signalling between endothelial cells and cardiac cells. Cardiovasc Res. 2014; 102:249–257. [PubMed: 24591150]
15. Huang P. Mouse models of nitric oxide synthase deficiency. J Am Soc Nephrol. 2000; 11:S120–S123. [PubMed: 11065342]
16. Gyurko R, Kuhlencordt P, Fishman M, Huang P. Modulation of mouse cardiac function in vivo by eNOS and ANP. Am J Physiol Heart Circ Physiol. 2000; 278:H971–H981. [PubMed: 10710367]
17. Champion H, Georgakopoulos D, Takimoto E, Isoda T, Wang Y, Kass D. Modulation of in vivo cardiac function by myocyte-specific nitric oxide synthase-3. Circ Res. 2004; 94:657–663. [PubMed: 14752030]
18. Bloch K, Janssens S. Cardiomyocyte-specific overexpression of nitric oxide synthase 3: impact on left ventricular function and myocardial infarction. Trends Cardiovasc Med. 2005; 15:249–253. [PubMed: 16226679]
19. Flaherty M, Brown M, Grupp I, Schultz J, Murphree S, Jones W. eNOS deficient mice develop progressive cardiac hypertrophy with altered cytokine and calcium handling protein expression. Cardiovasc Toxicol. 2007; 7:165–177. [PubMed: 17901560]
20. Brede M, Roell W, Ritter O, Wiesmann F, Jahns R, Haase A, et al. Cardiac hypertrophy is associated with decreased eNOS expression in angiotensin AT2 receptor-deficient mice. Hypertension. 2003; 42:1177–1182. [PubMed: 14581297]
21. Calderone A, Thaik CM, Takahashi N, Chang DL, Colucci WS. Nitric oxide, atrial natriuretic peptide, and cyclic GMP inhibit the growth-promoting effects of norepinephrine in cardiac myocytes and fibroblasts. J Clin Invest. 1998; 101:812–818. [PubMed: 9466976]
22. Ruetten H, Dimmeler S, Gehring D, Ihling C, Zeiher AM. Concentric left ventricular remodeling in endothelial nitric oxide synthase knockout mice by chronic pressure overload. Cardiovasc Res. 2005; 66:444–453. [PubMed: 15914109]
23. Ichinose F, Bloch KD, Wu JC, Hataishi R, Aretz HT, Picard MH, et al. Pressure overload-induced LV hypertrophy and dysfunction in mice are exacerbated by congenital NOS3 deficiency. Am J Physiol Heart Circ Physiol. 2004; 286:H1070–H1075. [PubMed: 14644766]
24. Buys ES, Raher MJ, Blake SL, Neilan TG, Graveline AR, Passeri JJ, et al. Cardiomyocyte-restricted restoration of nitric oxide synthase 3 attenuates left ventricular remodeling after chronic pressure overload. Am J Physiol Heart Circ Physiol. 2007; 293:H620–H627. [PubMed: 17416602]
25. Takimoto E, Champion HC, Li M, Ren S, Rodriguez ER, Tavazzi B, et al. Oxidant stress from nitric oxide synthase-3 uncoupling stimulates cardiac pathologic remodeling from chronic pressure load. J Clin Invest. 2005; 115:1221–1231. [PubMed: 15841206]
26. Zhao X, He G, Chen YR, Pandian RP, Kuppusamy P, Zweier JL. Endothelium-derived nitric oxide regulates postischemic myocardial oxygenation and oxygen consumption by modulation of mitochondrial electron transport. Circulation. 2005; 111:2966–2972. [PubMed: 15939832]
27. Zhao X, Chen YR, He G, Zhang A, Druhan LJ, Strauch AR, et al. Endothelial nitric oxide synthase (NOS3) knockout decreases NOS2 induction, limiting hyperoxygenation and conferring protection in the postischemic heart. Am J Physiol Heart Circ Physiol. 2007; 292:H1541–H1550. [PubMed: 17114245]
28. Chen YR, Chen CL, Pfeiffer DR, Zweier JL. Mitochondrial Complex II in the Post-ischemic Heart: OXIDATIVE INJURY AND THE ROLE OF PROTEIN S-GLUTATHIONYLATION. J Biol Chem. 2007; 282:32640–32654. [PubMed: 17848555]
29. Lee H, Chen C, Yeh S, Zweier J, Chen Y. Biphasic modulation of the mitochondrial electron transport chain in myocardial ischemia and reperfusion. Am J Physiol Heart Circ Physiol. 2012; 302:H1410–H1422. [PubMed: 22268109]
30. Redfearn ER, Whittaker PA. The determination of the oxidation-reduction states of ubiquinone (coenzyme Q) in rat-liver mitochondria. Biochimica et biophysica acta. 1966; 118:413–418. [PubMed: 4289837]
31. Yeh S, Lee H, Aune S, Chen C, Chen Y, Angelos M. Preservation of mitochondrial function with cardiopulmonary resuscitation in prolonged cardiac arrest in rats. Journal of molecular and cellular cardiology. 2009; 47:789–797. [PubMed: 19751739]

32. Duling DR. Simulation of multiple isotropic spin-trap EPR spectra. J Magn Reson B. 1994; 104:105–110. [PubMed: 8049862]
33. Lindorff-Larsen K, Winther JR. Thiol alkylation below neutral pH. Anal Biochem. 2000; 286:308–310. [PubMed: 11067758]
34. Griffith OW. Determination of glutathione and glutathione disulfide using glutathione reductase and 2-vinylpyridine. Anal Biochem. 1980; 106:207–212. [PubMed: 7416462]
35. Gardner PR, Fridovich I. Superoxide sensitivity of the Escherichia coli aconitase. J Biol Chem. 1991; 266:19328–19333. [PubMed: 1655783]
36. Gardner PR, Fridovich I. Inactivation-reactivation of aconitase in Escherichia coli. A sensitive measure of superoxide radical. J Biol Chem. 1992; 267:8757–8763. [PubMed: 1315737]
37. Gardner PR, Nguyen DD, White CW. Aconitase is a sensitive and critical target of oxygen poisoning in cultured mammalian cells and in rat lungs. Proc Natl Acad Sci U S A. 1994; 91:12248–12252. [PubMed: 7991614]
38. Vasquez-Vivar J, Kalyanaraman B, Kennedy MC. Mitochondrial aconitase is a source of hydroxyl radical. An electron spin resonance investigation. J Biol Chem. 2000; 275:14064–14069. [PubMed: 10799480]
39. Suda O, Tsutsui M, Morishita T, Tanimoto A, Horiuchi M, Tasaki H, et al. Long-term treatment with N(omega)-nitro-L-arginine methyl ester causes arteriosclerotic coronary lesions in endothelial nitric oxide synthase-deficient mice. Circulation. 2002; 106:1729–1735. [PubMed: 12270870]
40. Zhao H, Shimokawa H, Uragami-Harasawa L, Igarashi H, Takeshita A. Long-term vascular effects of Nomega-nitro-L-arginine methyl ester are not soley mediated by inhibition of endothelial nitric oxide synthesis in the rat mesenteric artery. J Cardiovasc Pharmacol. 1999; 33:554–566. [PubMed: 10218725]
41. Kang PT, Yun J, Kaumaya PP, Chen YR. Design and use of peptide-based antibodies decreasing superoxide production by mitochondrial complex I and complex II. Biopolymers. 2011; 96:207–221. [PubMed: 20564035]
42. Clementi E, Brown GC, Feelisch M, Moncada S. Persistent inhibition of cell respiration by nitric oxide: crucial role of S-nitrosylation of mitochondrial complex I and protective action of glutathione. Proc Natl Acad Sci U S A. 1998; 95:7631–7636. [PubMed: 9636201]
43. Chen YR, Chen CL, Yeh A, Liu X, Zweier JL. Direct and indirect roles of cytochrome b in the mediation of superoxide generation and NO catabolism by mitochondrial succinate-cytochrome c reductase. J Biol Chem. 2006; 281:13159–13168. [PubMed: 16531408]
44. Shiva S, Brookes PS, Patel RP, Anderson PG, Darley-Usmar VM. Nitric oxide partitioning into mitochondrial membranes and the control of respiration at cytochrome c oxidase. Proc Natl Acad Sci U S A. 2001; 98:7212–7217. [PubMed: 11416204]
45. Hudlicka O, Brown M, Egginton S. Angiogenesis in skeletal and cardiac muscle. Physiol Rev. 1992; 72:369–417. [PubMed: 1372998]
46. Barouch LA, Harrison RW, Skaf MW, Rosas GO, Cappola TP, Kobeissi ZA, et al. Nitric oxide regulates the heart by spatial confinement of nitric oxide synthase isoforms. Nature. 2002; 416:337–339. [PubMed: 11907582]
47. Chen YR, Zweier JL. Cardiac mitochondria and reactive oxygen species generation. Circ Res. 2014; 114:524–537. [PubMed: 24481843]
48. Le Gouill E, Jimenez M, Binnert C, Jayet PY, Thalmann S, Nicod P, et al. Endothelial nitric oxide synthase (eNOS) knockout mice have defective mitochondrial beta-oxidation. Diabetes. 2007; 56:2690–2696. [PubMed: 17682093]
49. Muller FL, Liu Y, Van Remmen H. Complex III releases superoxide to both sides of the inner mitochondrial membrane. J Biol Chem. 2004; 279:49064–49073. [PubMed: 15317809]
50. Dikalov SI, Harrison DG. Methods for detection of mitochondrial and cellular reactive oxygen species. Antioxid Redox Signal. 2014; 20:372–382. [PubMed: 22978713]
51. Mieyal JJ, Gallogly MM, Qanungo S, Sabens EA, Shelton MD. Molecular mechanisms and clinical implications of reversible protein S-glutathionylation. Antioxid Redox Signal. 2008; 10:1941–1988. [PubMed: 18774901]

52. Gallogly MM, Mieyal JJ. Mechanisms of reversible protein glutathionylation in redox signaling and oxidative stress. Curr Opin Pharmacol. 2007; 7:381–391. [PubMed: 17662654]

53. Kang PT, Chen CL, Ren P, Guarini G, Chen YR. BCNU-induced gR2 defect mediates S-glutathionylation of Complex I and respiratory uncoupling in myocardium. Biochem Pharmacol. 2014; 89:490–502. [PubMed: 24704251]

54. Chen CL, Chen J, Rawale S, Varadharaj S, Kaumaya PP, Zweier JL, et al. Protein tyrosine nitration of the flavin subunit is associated with oxidative modification of mitochondrial complex II in the postischemic myocardium. J Biol Chem. 2008; 283:27991–28003. [PubMed: 18682392]

55. Detweiler CD, Deterding LJ, Tomer KB, Chignell CF, Germolec D, Mason RP. Immunological identification of the heart myoglobin radical formed by hydrogen peroxide. Free radical biology & medicine. 2002; 33:364–369. [PubMed: 12126758]

56. Chen YR, Chen CL, Zhang L, Green-Church KB, Zweier JL. Superoxide generation from mitochondrial NADH dehydrogenase induces self-inactivation with specific protein radical formation. J Biol Chem. 2005; 280:37339–37348. [PubMed: 16150735]

- Complex I S-glutathionylation is mediated by protein thiyl radicals and GSH.
- eNOS deletion impairs mitochondrial function and increases pro-oxidant activity.
- Deletion of eNOS induces a more oxidized physiological setting in the murine heart.
- Complex I thiyl radicals and S-glutathionylation are enhanced in eNOS$^{-/-}$ heart.
- Cardiac-specific overexpression of SOD2 diminishes Complex I thiyl radicals.

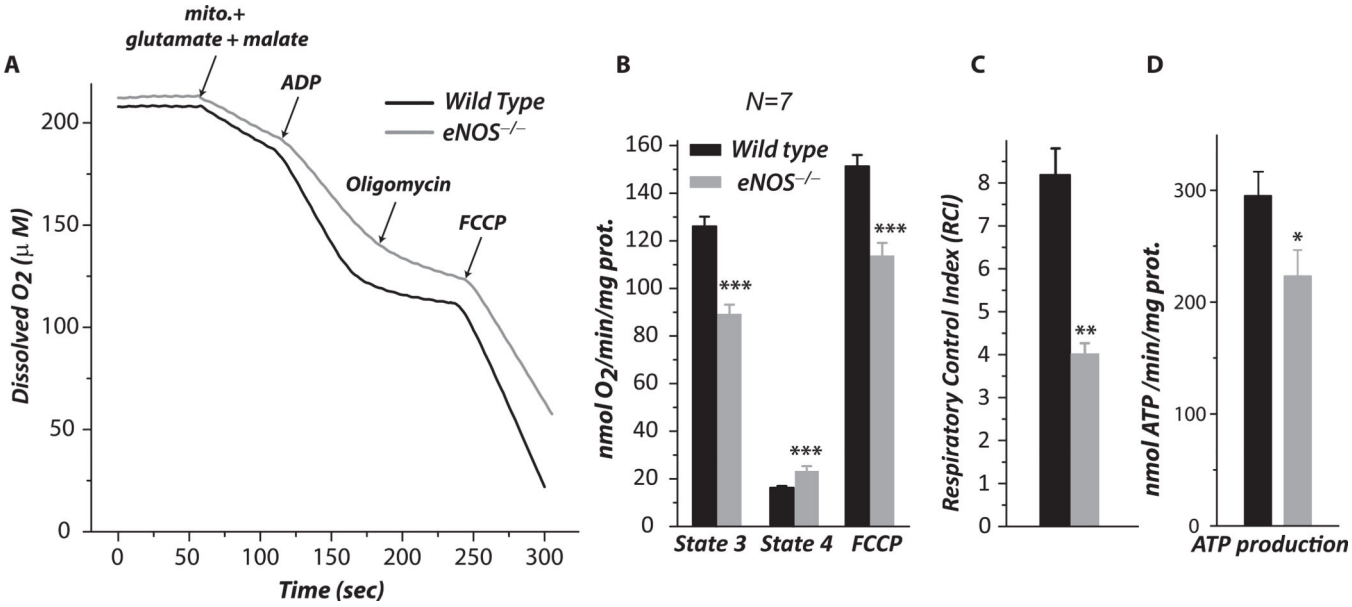

Fig. 1.

Mitochondria were prepared from the myocardia of wild type and eNOS$^{-/-}$ mice, and then subjected to measurement of the oxygen consumption rate (OCR) by oxygen polarography at 30 °C as described under "Material and Methods". ***A–B,*** state 2, state 3, state 4, and FCCP-mediated OCRs from the isolated mitochondria. ***C,*** Respiratory control index (RCI) obtained from the ratio of state 3 OCR to state 4 OCR. $n = 7$; **p <0.01 and ***p < 0.001, assessed by student's t-test between WT control and eNOS$^{-/-}$ in ***B*** and ***C***. Comparison among three groups of OCR (state 3, state 4, and FCCP) in ***B*** was analyzed by one-way ANOVA followed by Tukey's HSD test, indicating significant difference among the three groups of wild type and three groups of eNOS$^{-/-}$ ($p < 0.001$). Data were normalized to the amount (mg) of mitochondrial protein in ***B*** and ***D***.

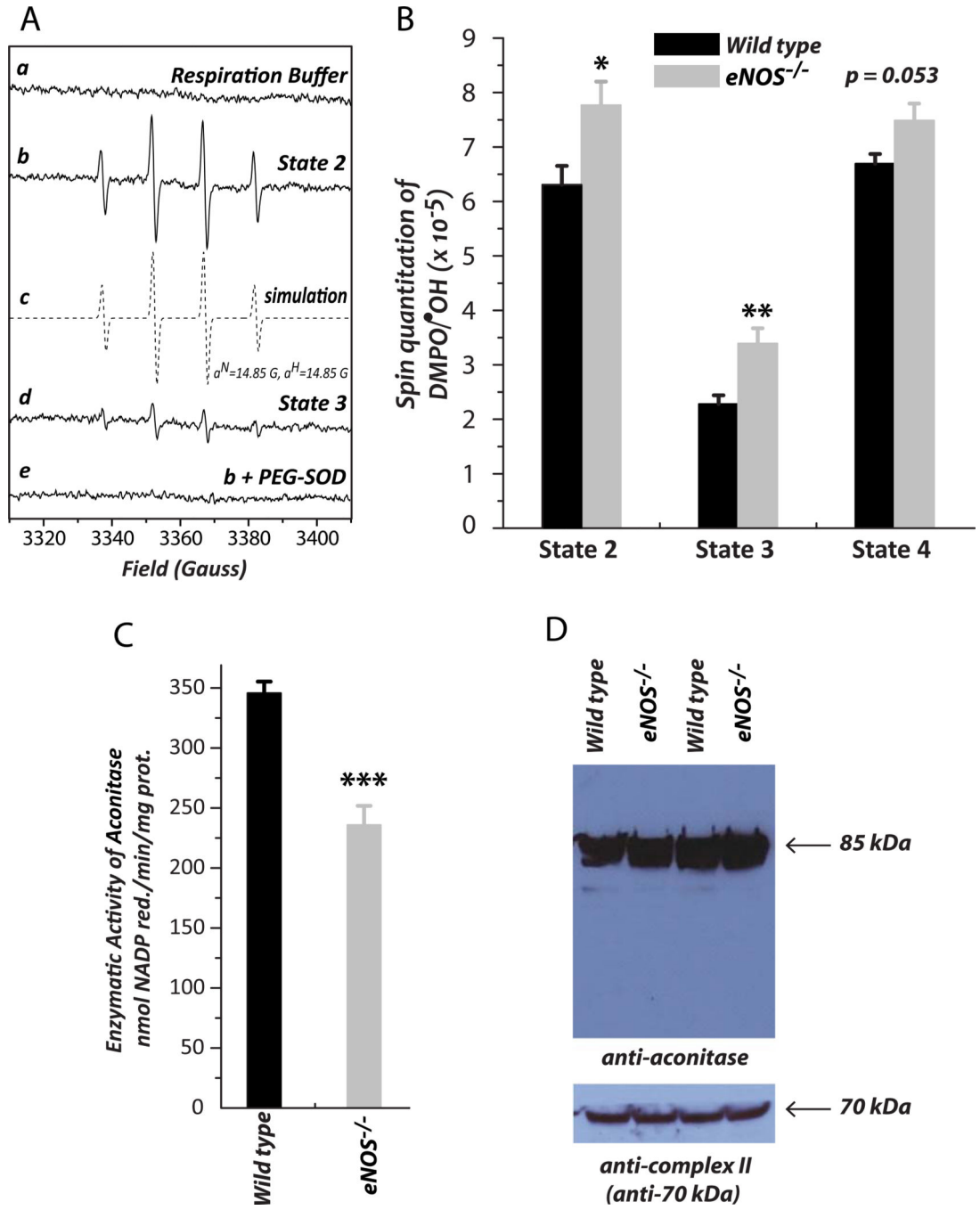

Fig. 2.

$^{\bullet}O_2^-$ generation mediated by mitochondria in the presence of glutamate and malate (NADH-linked) was assessed by EPR spin trapping with DMPO according to our published methods [7]. ***A*** is the EPR spectra of the SOD-sensitive DMPO/$^{\bullet}$OH adduct under the conditions of state 2 *(b)*, the spectrum obtained from computer simulation *(c)*, state 3 *(d)*, and the effect of PEG-SOD on the detected DMPO/$^{\bullet}$OH adducts *(e)*. The EPR spectra obtained under the conditions of state 4 and chemical uncoupling with FCCP were not shown. PEG-SOD, polyethylene glycol covalently linked to superoxide dismutase. ***B*** is the quantitative analysis

of DMPO/$^{\bullet}$OH adducts produced under the conditions of various respiratory statuses in ***A***. The spin quantitation for each spectrum was obtained by double integration of the simulation spectrum as described in a previous publication [7] (n = 6; *p <0.05 and **p < 0.01, assessed by student's t-test between WT control and eNOS$^{-/-}$). Comparison among four groups of $^{\bullet}O_2^-$ generation at state 2, state 3, and state 4, conditions in ***B*** was analyzed by one-way ANOVA followed by Tukey's HSD test, indicating significant difference between state 2 and state 3; state 3 and state 4 (n = 6, p < 0.001). ***C,*** the isolated mitochondria were permeabilized by alamethicin (40 μg protein : 1 μg alamethicin ratio), and then subjected to the aconitase activity assay as described in "Material and Methods". ***D***, mitochondrial preparation (100 μg protein per lane) was probed with a polyclonal antibody against aconitase (1:500) and the 70 kDa subunit of Complex II (1:30,000) was used as the loading control. Data were normalized to the amount (mg) of mitochondrial protein in ***B*** and ***C***.

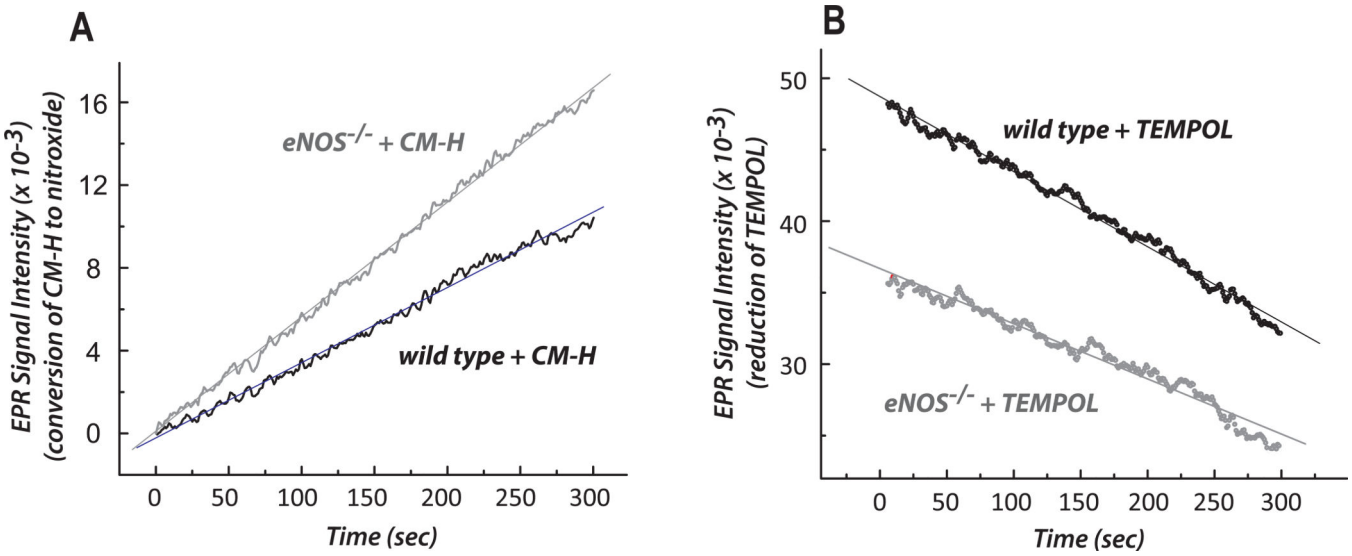

Fig. 3. The redox activities of the myocardium from wild type and eNOS$^{-/-}$ were measured by EPR with the spin probes of CM-H (*in A*) and TEMPOL (*in B*)

Conversion of CM-H to stable nitroxide was measured by EPR at 298K in tissue homogenates (0.25 mg/mL) of wild type or eNOS$^{-/-}$ myocardium in SHE buffer (250 mM sucrose, 10 mM HEPES, and 1 mM EDTA, pH 7.4) containing 1 mM DTPA and 1 mM CM-H (in ***A***) or TEMPOL (in ***B***). The instrumental settings used for detecting the three-line spectrum of the nitroxide formed were: center field, 3360.3 G; sweep width, 60 G; microwave frequency, 9.43 GHz; power, 20 mW; receiver gain, 5.02×10^3; modulation frequency, 100kHz; modulation amplitude, 1 G; time constant, 163.84 ms; conversion time, 41 ms; sweep time, 42 sec; number of X-scans, 1. The parameters for the kinetic mode were: static field, 3360.3 G; receiver gain, 2×10^3; time constant, 2624.44 ms; conversion time, 1,000 ms; and sweep time, 300s; number of scans, 1. The CM-H oxidation experiment was performed three times ($n=3$) for calculating redox activity.

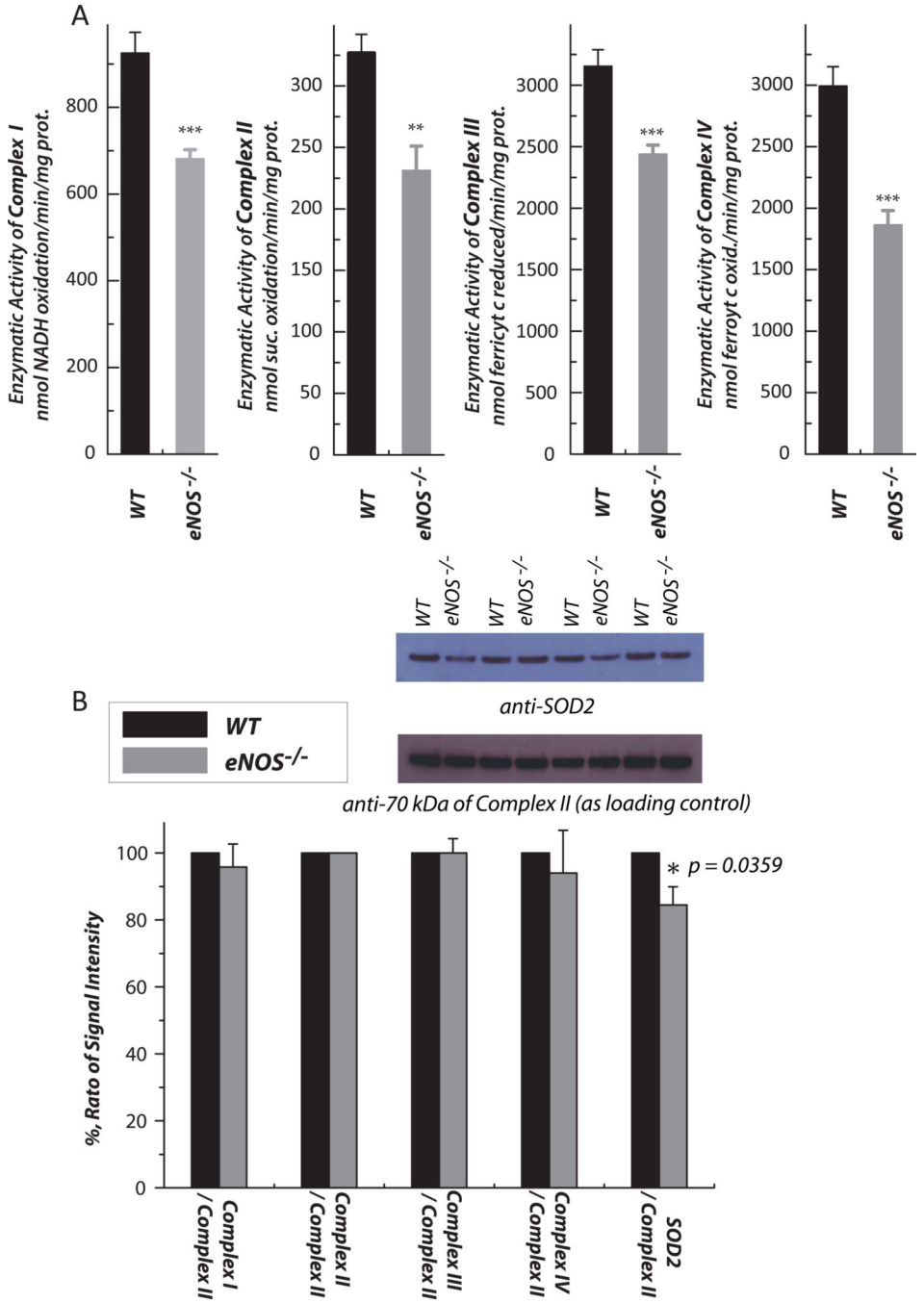

Fig. 4.

Hearts were removed from wild type and eNOS$^{-/-}$ mice, and subjected to mitochondrial preparation. ***A,*** enzymatic activities of electron transport chain (ETC) components in the mitochondria were assayed as described previously (n = 7). ***B***, Protein expression of ETC components and SOD2 in the mitochondria was assessed by Western blot using the following antibodies: Ab51 for Complex I (1:10,000)[6], AbGSC90 for Complex II (1:30,000) [54], the monoclonal antibody against Rieske iron-sulfur protein (1:1000) and Cox I (1:3000) for Complexes III and IV, and a polyclonal antibody against SOD2 (1:2000).

The protein expression level of subunit I (70 kDa flavoprotein) of Complex II in the mitochondria was used as a loading control. The density ratio of the blotting signals between the ETC components/SOD2 and Complex II was quantitated by software Image J. $n = 4$; *p < 0.05, **p < 0.01, ***p < 0.001. Data were normalized to the amount (mg) of mitochondrial protein in ***A***.

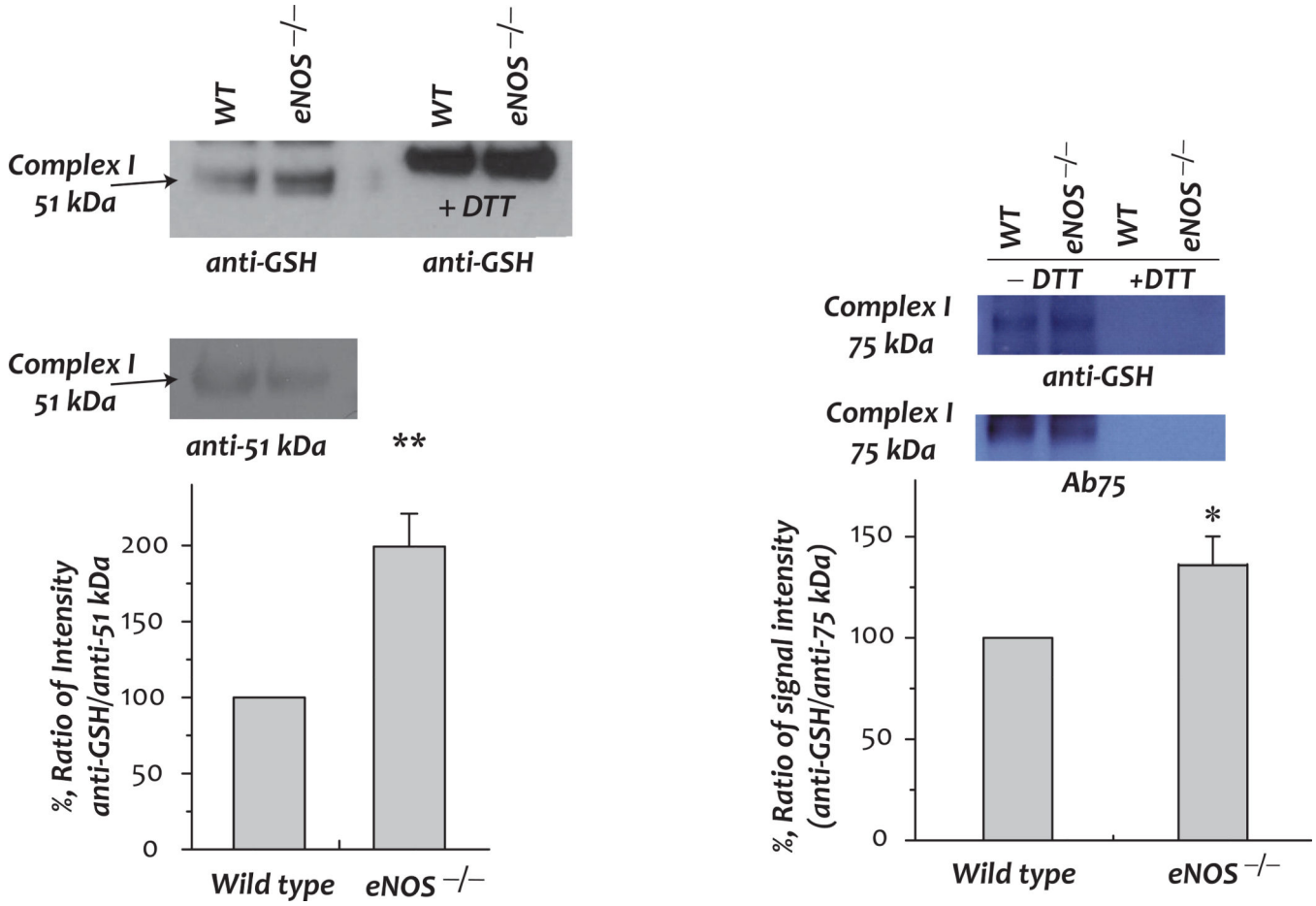

Fig. 5. Protein S-glutathionylation of the 51 kDa and 75 kDa subunits of Complex I in myocardial mitochondria and the effect of eNOS knockout

A mitochondrial preparation (1 mg protein used per IP) was subjected to immunoprecipitation (IP) with Ab51 and Ab75 (Ab against 51 kDa and 75 kDa in [6, 41] respectively), and subsequently subjected to SDS-PAGE and immunoblotted with anti-GSH monoclonal antibody (1:500, upper panel). Blottings on the nitrocellulose membrane were probed with Ab 51 (1:10,000) and Ab75 (1:5000) to quantitate the protein of the 51 kDa and 75 kDa subunits. The density ratios of signals were quantitated by software Image J (NIH) (n = 3, * p <0.01).

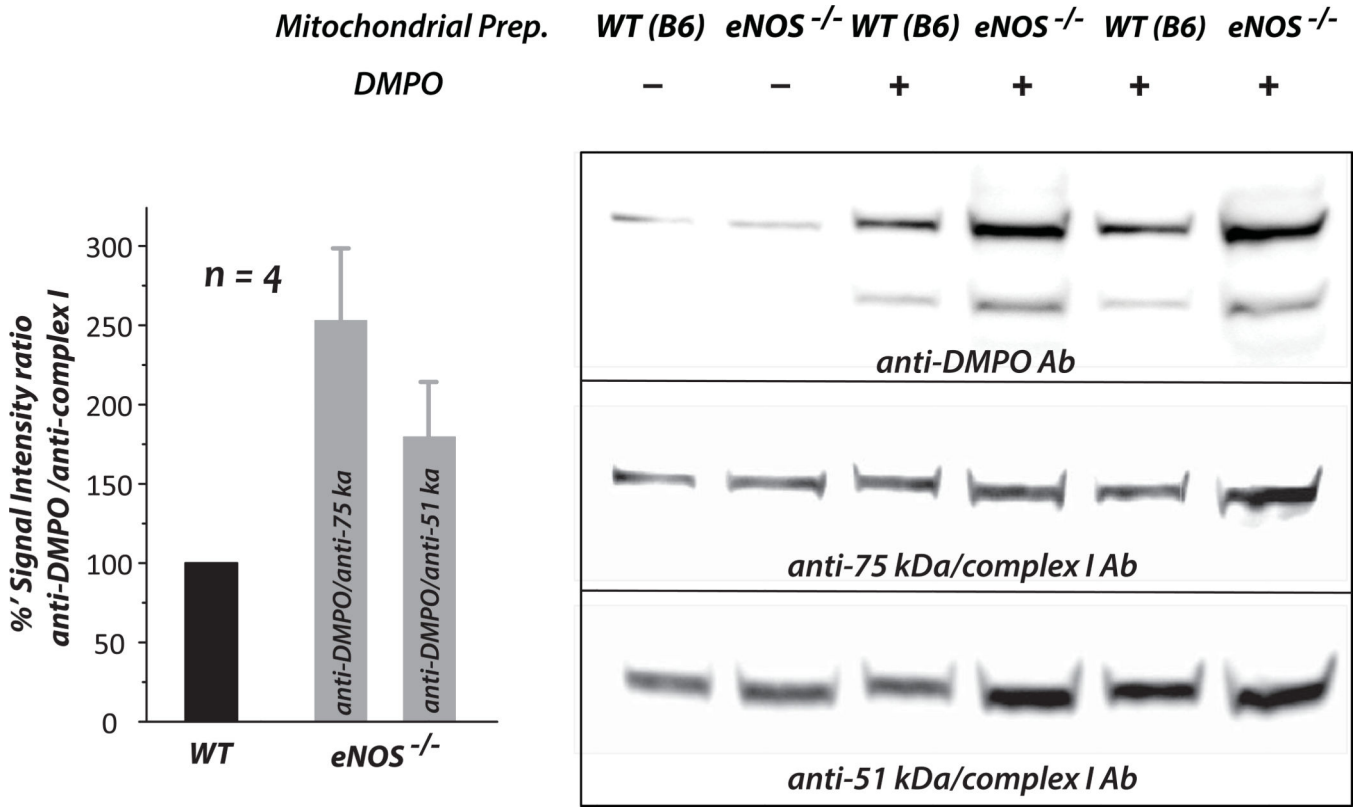

Fig. 6. Detection of protein-centered radicals formed at the 51 kDa and 75 kDa subunits of Complex I by immuno-spin trapping, and the effect of eNOS knockout on the formation of Complex I-derived protein radicals in myocardial mitochondria

Mitochondrial preparations (1 mg/mL) were incubated with the spin trap DMPO (200 mM) at 37 °C for 5 min, and 100 μg protein per lane subjected to SDS-PAGE and immunoblotting with an anti-DMPO polyclonal antibody (1:1000) [7, 55, 56]. Protein expression levels of the 51 kDa and 75 kDa subunits of Complex I in mitochondria were re-probed with Ab51 (1:10,000) and Ab75 (1:5000). The signals of DMPO adducts were normalized to those of the Complex I 51 kDa and 75 kDa subunits respectively. (n = 4, *$p < 0.05$ and **$p < 0.01$).

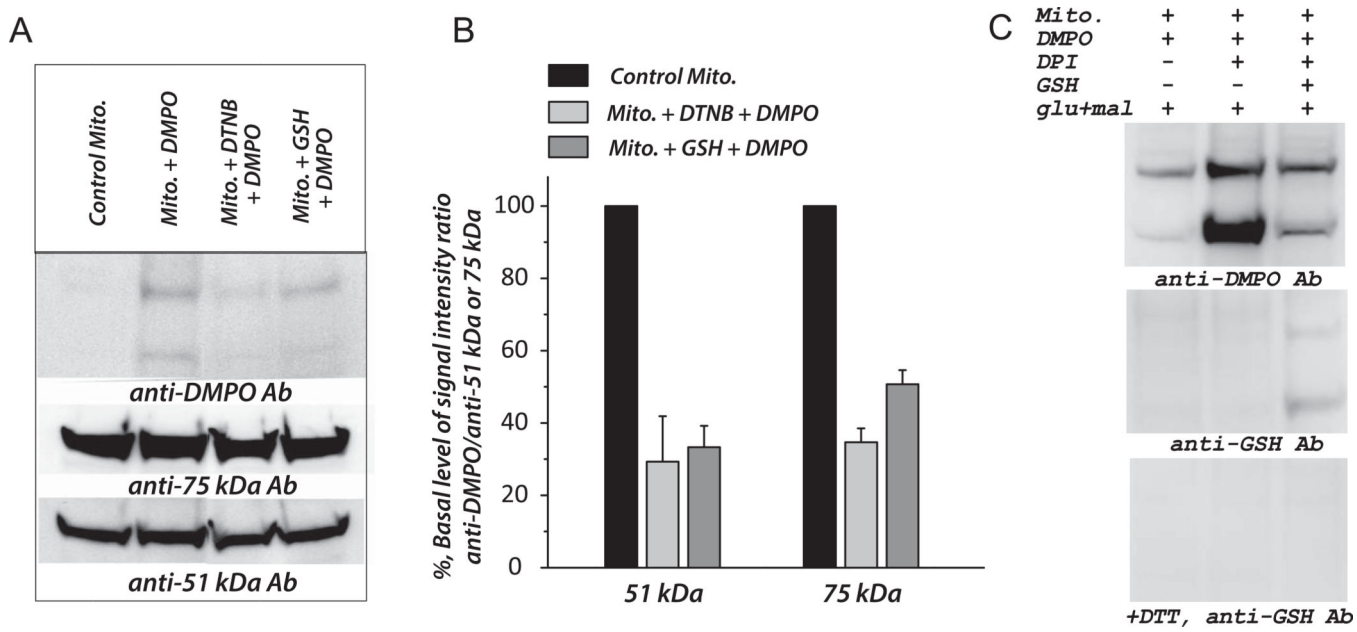

Fig. 7. Effect of DTNB *(Ellman's reagent)* and GSH on the formation of DMPO protein radical adducts at the 51kDa and 75 kDa subunits of mitochondrial Complex I

A–B, Mitochondria (0.83 mg/ml) isolated from mouse heart (wild type) was pre-incubated with DTNB (1 mM) or GSH (1 mM) at room temperature for 10 min. DTNB-treated or GSH-treated mitochondria were subjected to immunospin trapping analysis with anti-DMPO antibody (1:1000) and normalized to the Western signals with Ab51 (1:10,000) and Ab75 (1:5000) as described in the legend of Fig. 6. **C,** Mitochondria were pre-incubated with DPI (1 mM) at RT for 10 min, and the reaction was initiated with glutamate (70 mM) plus malate (2.5 mM). The reaction mixture was incubated at 37 °C for 5 min. Aliquots (120 μg protein per lane) of mixture were withdrawn for SDS-PAGE, and immunoblotted with anti-DMPO antibody (1:1000, upper panel) and anti-GSH antibody (1:500) with (lower panel) or without (middle panel) dithiothreitol (DTT). The experiment was performed three times (*n=3*).

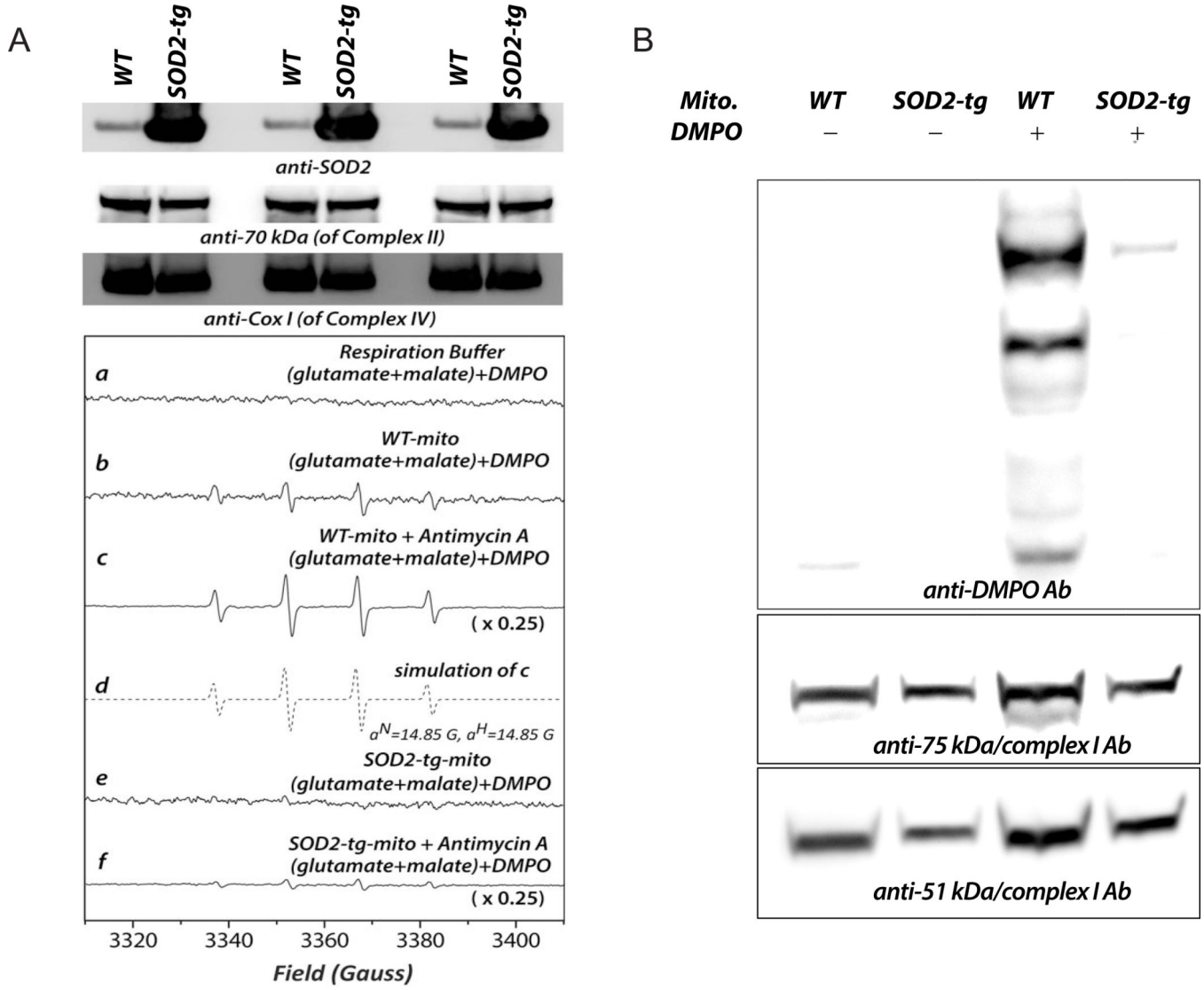

Fig. 8. Cardiac-specific SOD2 overexpression diminished $^{\bullet}O_2^-$ in mitochondria and the formation of protein radicals on mitochondrial Complex I

Hearts were removed from cardiac-specific SOD2 transgenic (SOD2-tg) and wild type mice (FVB/NJ strain), and subjected to mitochondrial preparation and immunoblotting using anti-SOD2 antibody (1:2000), an antibody against the 70 kDa subunit of complex II (1:30,000), and anti-Cox I antibody (1:3000, upper panel *in* ***A***). Lower panel in ***A,*** *b* and *e*: $^{\bullet}O_2^-$ generation mediated by mitochondria isolated from murine hearts of wild type and SOD2-tg mice, respectively; *c* and *f*: the same as *b* and *e*, except that antimycin A (10 μM) was included in the system. ***B,*** Immuno-spin trapping analysis of protein radical adducts of mitochondrial Complex I was conducted according to the approach described in the legend of Fig. 5. The experiment was performed four times (*n=4*).

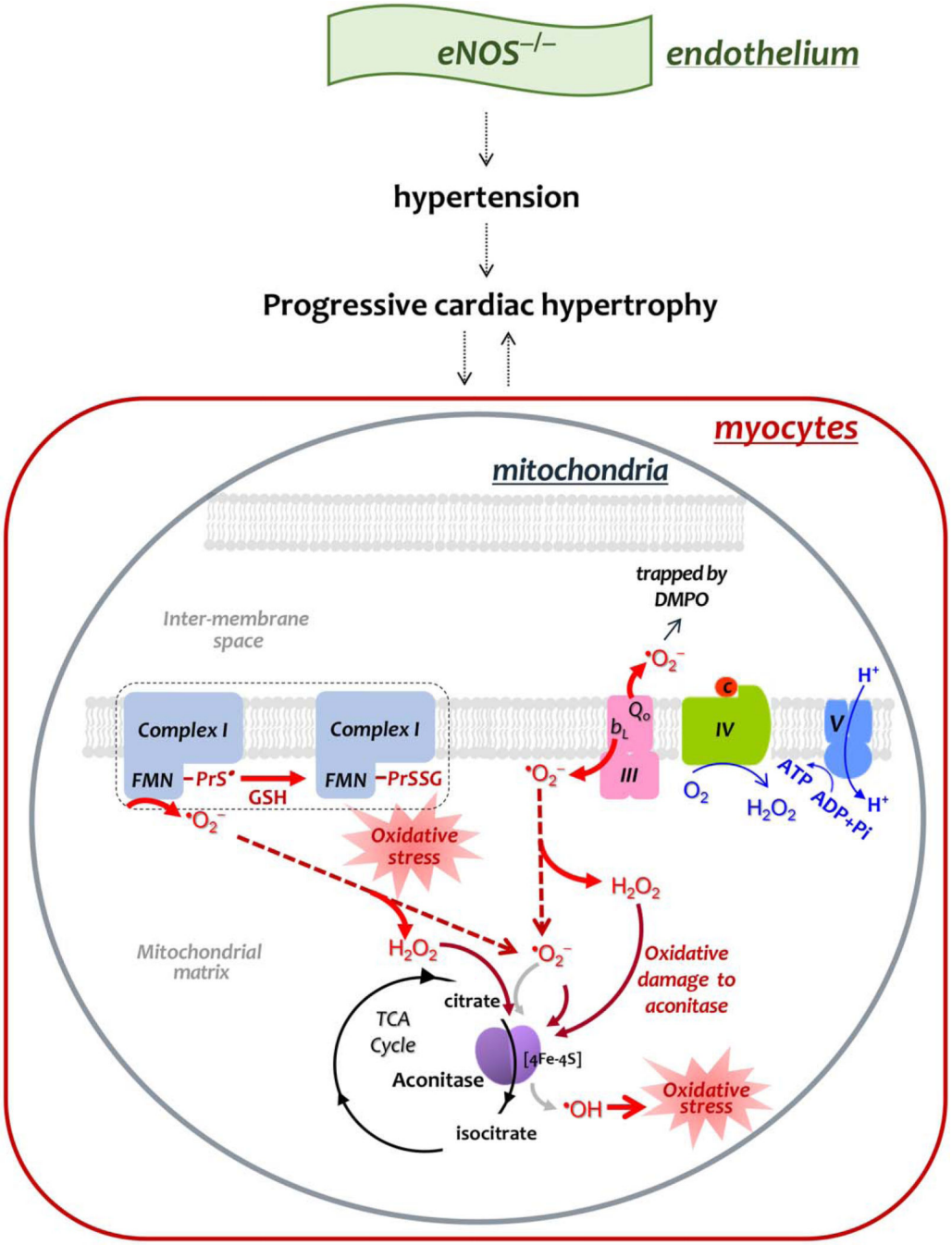

Fig. 9. Diagram showing the effect of eNOS knockout on the mitochondrial function of the mouse heart, and mechanism-based S-glutathionylation of Complex I

In comparison to the basal conditions, genetic deletion of eNOS impairs EDRF-mediated vasodilation, leading to the phenotype of hypertension, and inducing progressive hypertrophy. The phenotype of progressive cardiac remodeling is likely mediated by elevation of mitochondrial oxidative stress in myocytes or vice versa. Increased oxidative stress decreases the coupling of oxygen consumption with OXPHOS for ATP synthesis (indicated by *fine blue arrows* in Complex IV and Complex V), which would further

increase electron leakage for $^{\bullet}O_2^-$ production (indicated by *thick red arrows*). Increased $^{\bullet}O_2^-$ production by Complexes I and III damages the 4Fe-4S cluster of aconitase in the TCA cycle (*thick* brick arrows and black cycle), and increases pro-oxidant activity of aconitase to generate •OH (coarse gray arrow), augmenting oxidative stress. Enhanced $^{\bullet}O_2^-$ production also facilitates Complex I-derived protein thiyl radical formation (Pr$S^{\bullet}$), which mediates enhanced S-glutathionylation (PrSSG) of Complex I (*denoted by dashed closed bracket*).

Table I

Level of GSH pool in the cytosolic compartment and mitochondria from the myocardium of wild type and eNOS$^{-/-}$ mice.

	[GSH] + [GSSG] (nmol/mg prot.)	[GSSG] (nmol/mg prot.)	[GSH]/[GSSG]
Cytosol/WT	**16.24±0.27**	**0.513±0.029**	**31.63**
Cytosol/eNOS$^{-/-}$	**17.37±0.77**	**0.581±0.041**	**29.87**
Cytosol/WT + L-NAME	**16.62±0.62**	**0.737±0.053*****	**22.54**
Mitochondria/WT	**3.32±0.10**	**0.104±0.006**	**31.84**
Mitochondria/eNOS$^{-/-}$	**3.62±0.09***	**0.138±0.010****	**26.22**
Mitochondria/WT + L-NAME	**3.47±0.10**	**0.128±0.005***	**27.21**

*** p<0. 001 (n= 8), compared with Cytosol/WT;

** p<0.01 (n=8), compared with Mitochondria/WT,

* p<0.05 (n=8), compared with Mitochondria/WT.